

# Bismuth (III) Telluride ( $\text{Bi}_2\text{Te}_3$ ) Based Topological Insulator Embedded in PVA as Passive Saturable Absorber in Erbium-Doped Fiber Laser

N H M Apandi<sup>1\*</sup>, F Ahmad<sup>1</sup>, S Ambran<sup>1</sup>, M Yamada<sup>1</sup> and S W Harun<sup>2</sup>

<sup>1</sup>Dept. of Electronic Systems Engineering, Malaysia-Japan International Institute of Technology, Universiti Teknologi Malaysia, Jalan Sultan Yahya Petra, 54100, Kuala Lumpur, Malaysia

<sup>2</sup>Photonic Research Center, University of Malaya, 50603 Kuala Lumpur, Malaysia

Email: \*nurhidayahapandi@gmail.com

**Abstract.** We demonstrate a passive Q-switched by integrating a Bismuth (III) Telluride ( $\text{Bi}_2\text{Te}_3$ ) dispersed in Polyvinyl Alcohol (PVA) as passive saturable absorber. The experimental works show that the proposed passive saturable absorber operated at input power ranging from 21.69 mW to 126.89 mW with central operating wavelength of 1531 nm. We observe the tunable repetition rate from 40 kHz to 166 kHz with the shortest pulse width of 1.32  $\mu\text{s}$ . The laser produced maximum instantaneous output peak power and pulse energy of 1.62 mW and 11.2 nJ, respectively. The signal to noise ratio was measured at 49 dB which indicates the stability of the generated pulse.

## 1. Introduction

In the past years, the study in using real saturable absorbers have become crucial for researchers to generate pulsed laser. Fiber lasers has been regarded as the most promising laser configuration as it is proven to be superior than other type of lasers such as dye, gas, chemical, solid state and semiconductor lasers. The first laser was successfully demonstrated by Maiman in 1960. A few years later, the Q-switched laser was discovered by using colored glass filter and dyes onto ruby laser configuration [1]. Since then, the materials used has evolved from semiconductor saturable absorber mirror (SESAM) to nanomaterials such as quantum dots, carbon nanotubes, graphene, transition metal dichalcogenides (TMDs), black phosphorous (BP) and topological insulators (TIs) [2]. Topological insulators in bulk state have an insulating energy gaps whether in two or three dimensions but the sample boundary were protected by time-reversal symmetry at the surface state or gapless edge [3]. These TIs are robust and have a simple surface states consisting of a single Dirac cone and these stoichiometric crystals are Bismuth (III) Telluride ( $\text{Bi}_2\text{Te}_3$ ), Bismuth (III) Selenide ( $\text{Bi}_2\text{Se}_3$ ) and Antimony (III) Telluride ( $\text{Sb}_2\text{Te}_3$ ). Basically,  $\text{Bi}_2\text{Te}_3$  share the same rhombohedral crystals structure with five atoms in one unit cell thus the material is known as quintuple layers along the z-axis [3]. Each of the quintuple layer consists of five atoms with two equivalent Te atoms. The atoms was covalently bonded with stacks of Te-Bi-Te-Bi-Te within each layer where the layers (quintuple layer) were held together by van der Waals forces as shown in Figure 1 [4].



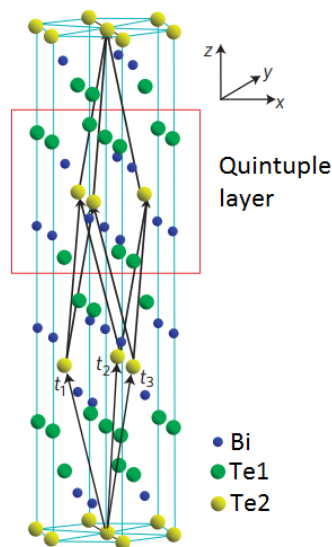


**Figure 1.** Crystal structure of Bi<sub>2</sub>Te<sub>3</sub> with three primitive lattice vectors denoted as  $t_{1,2,3}$  and a quintuple layer as indicated by the red square [3]

Experimentally, the first demonstration of passive saturable absorber (SA) of Bi<sub>2</sub>Te<sub>3</sub> for ultrafast fiber laser has been done by drop casting technique on a quartz plate [5]. Since that, the integration of the SA is approached either by evanescent wave interaction [6-9], sandwiching [7-8] or free space coupling [10] with a wider operating wavelength from 1  $\mu\text{m}$  to 3  $\mu\text{m}$  [6-10]. The TI based passive SA application has been reported by Chen *et al.* [7] and Wu *et al.* [8] by using Bi<sub>2</sub>Te<sub>3</sub>. Chen *et al.* [7] synthesized a layer of Bi<sub>2</sub>Te<sub>3</sub> nano-sheets by liquid phase exfoliation (LPE) and then dissolved in isopropyl alcohol. The Bi<sub>2</sub>Te<sub>3</sub> based SA was attached at the fiber end-facet after optical deposition method with central wavelength of 975 nm and maximum power of 500 mW. The central wavelength tunable from 1510.9 nm to 1589.1nm, with a large energy of 1.5  $\mu\text{J}$ , range of repetition rate from 2.2 kHz to 12.8 kHz, and the shortest pulse width 13  $\mu\text{s}$  is reported. The signal-to-noise ratio is 36.4dB. Wu *et al.* [8] also synthesized the TI nanomaterial by using liquid exfoliation approach before it is dispersed in isopropyl alcohol. The Bi<sub>2</sub>Te<sub>3</sub> nano-sheets were then deposited onto the fiber end-facet with a pump power of 80 mW and central wavelength of 975 nm. The generated pulse recorded maximum pulse energy of 7.5 nJ, range of repetition rate from 12.6 kHz to 177.7 kHz, shortest pulse width of 0.2  $\mu\text{s}$ , and signal-to-noise ratio of 47 dB. The use of optical deposition method is not efficient for scalable production of SA, the process is time consuming and the thickness is uncontrollable. On the contrary, this work proposes a simpler approach in developing Bi<sub>2</sub>Te<sub>3</sub>-PVA film as passive SA at 1.5  $\mu\text{m}$ . The generated Q-switched pulse operated at a central wavelength of 1531 nm, tunable repetition rate from 40 kHz to 166 kHz with the shortest pulse width of 1.32  $\mu\text{s}$ . The laser produces maximum instantaneous output peak power and pulse energy of 1.62 mW and 11.2 nJ, respectively.

## 2. Methodology

Bismuth (III) Telluride (Bi<sub>2</sub>Te<sub>3</sub>) powder (Sigma Aldrich) characterized with -325 mesh and 99.99% trace metals basis with molecular weight of 800.76g/mol was used per received. To prepare the host polymer, 1 g of PVA (Sigma Aldrich) was dissolved in 120 ml de-ionized (DI) water with the aid of a magnetic stirrer at room temperature. TI based passive SA film was prepared by mixing 14 mg of Bi<sub>2</sub>Te<sub>3</sub> with 3 ml of PVA suspension and thoroughly mixed with the aid of magnetic stirrer for three hours. Then the Bi<sub>2</sub>Te<sub>3</sub>-PVA suspension was placed in ultrasonic bath for one hour to make sure that the Bi<sub>2</sub>Te<sub>3</sub> powder was fully binded with the binder (PVA). After that, the suspension was carefully poured onto a petri dish to avoid any air bubble and was left at room temperature for 48 hours to

develop  $\text{Bi}_2\text{Te}_3$ -PVA composite film. The developed film was characterized using FESEM as shown in Figure 2 and the figure clearly shows that the  $\text{Bi}_2\text{Te}_3$  powder was thoroughly mixed with PVA host polymer. The transmission characteristics of the developed film were further measured using a UV-VIS-NIR spectrophotometer (Perkin Elmer, Lambda 750) with pure PVA film as reference. Figure 3 shows the transmission spectrum of the fabricated  $\text{Bi}_2\text{Te}_3$ -PVA film and it shows the transmittance is at 21% at 1.5  $\mu\text{m}$  region. The film can also be investigated at 1  $\mu\text{m}$  and 2  $\mu\text{m}$  region showing the broadband properties of the  $\text{Bi}_2\text{Te}_3$  based passive SA as the structure of the TI is not affected by host polymer [11]. Figure 4 shows the Raman spectrum of the developed  $\text{Bi}_2\text{Te}_3$ -PVA film with low peak at  $\sim 62 \text{ cm}^{-1} (A_{1g}^1)$ ,  $\sim 95 (E_g^2)$  and  $11 (A_{1g}^2)$ , respectively. The low peak is maybe due to the low concentration of the Bismuth (III) Telluride powder in PVA and the effect of the film thickness [13]. The simple approach in this works to mix the  $\text{Bi}_2\text{Te}_3$  powder with PVA in room temperature for scalable production of  $\text{Bi}_2\text{Te}_3$  based SA is very attractive.

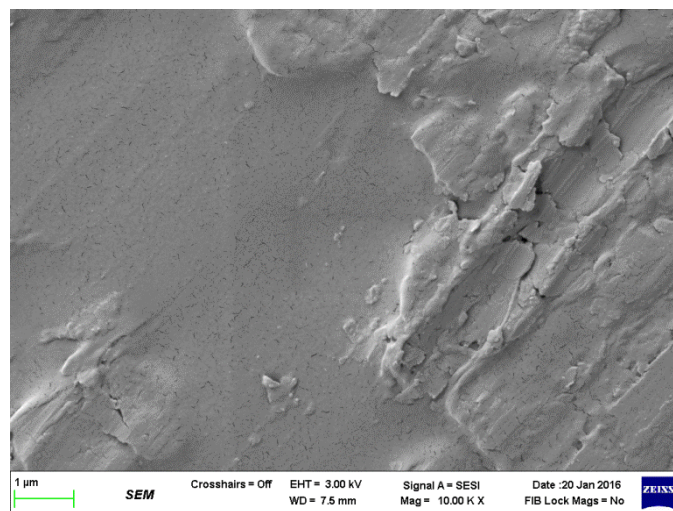


**Figure 2.** FESEM image of  $\text{Bi}_2\text{Te}_3$ -PVA film

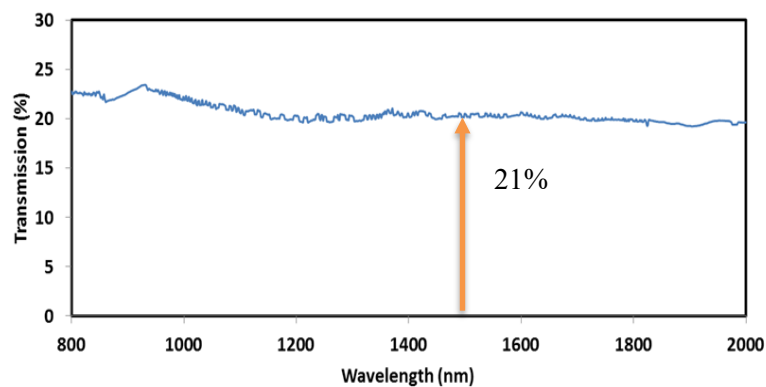


**Figure 3.** Transmission spectrum of  $\text{Bi}_2\text{Te}_3$ -PVA film

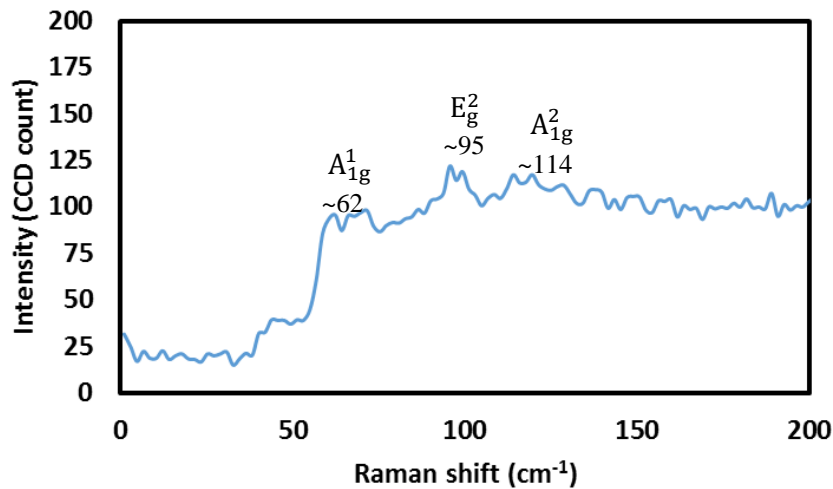


**Figure 4.** Raman spectrum of free standing  $\text{Bi}_2\text{Te}_3$ -PVA film

### 3. Experimental setup

In order to investigate the functionality of the prepared of  $\text{Bi}_2\text{Te}_3$ -PVA as passive saturable absorber, a small portion of the developed film was inserted into the fiber laser cavity. Figure 5 shows the schematic of the Q-switched fiber laser with the bismuth telluride based SA. The pump source is a laser diode (LD) with emission centered at 980 nm. A piece of 3 m long Erbium doped fiber (EDF) was used as the laser gain medium with absorption coefficient of 23 dB/m at 1550 nm. The pump was delivered into EDF via a 980/1550 fused wavelength division multiplexer (WDM). A polarization dependent isolator, placed after the EDF was used to ensure unidirectional operation and eliminate undesired feedback from the output end facet. A fused fiber optical coupler (OC) was used to extract 5% of the propagating light in the laser cavity, and then characterized as output. A saturable absorber was inserted by sandwiching the  $\text{Bi}_2\text{Se}_3$ -PVA sample between two pigtailed, and then placed within ring cavity. A 3 dB coupler was placed after the 95/5 OC to investigate the performance of the ring cavity by using an optical spectrum analyser (OSA) which is employed for the spectral analysis of the pulse in Erbium doped fiber laser, whereas the oscilloscope (OSC) is used to observe the output pulse train of the Q-switched operation via photo-detector. Radio frequency spectrum analyzer (RFSA) was used to measure the signal to noise ratio (SNR), while optical power meter was used to measure the average output power.

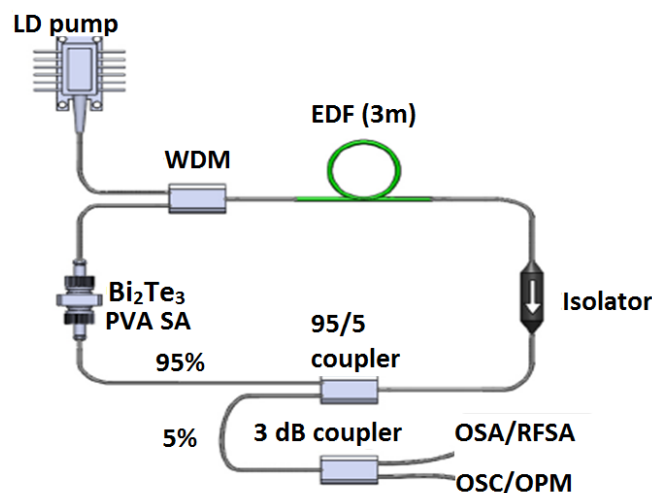


**Figure 5.** Experimental setup of the proposed passively Q-switched EDFL by residing  $\text{Bi}_2\text{Te}_3$ -PVA based passive saturable absorber

#### 4. Results and discussion

A stable Q-switched operation was obtained once the pump power exceeded a threshold of 21.69 mW. Figure 6 shows a typical optical spectrum with a central wavelength of 1531 nm and consist of parasitic continuous wave at 1530.64 nm. It has a 3 dB spectral bandwidth of 0.03 nm. The parasitic continuous wave laser is observed due to the reflection light interference from two fiber connectors' end [12]. The stable Q-switched pulse train has a repetition rate of 166 kHz higher than reported work [7,14], corresponding to a time interval between adjacent pulses of 6  $\mu$ s with maximum input power of 126 mW as shown in Figure 7. Figure 8 shows a zoom-in single pulse profile. The pulse has a symmetric intensity profile with a full width at half maximum (FWHM) of 1.32  $\mu$ s which is better than previous works [7,14]. Unlike the mode-locking operation where the repetition rate is determined by the cavity length, Q-switching laser has a tunable repetition rate that is dependent on the cavity gain, loss and cavity birefringence [7]. With the increasing pump power, more electrons can be excited and accumulated in the upper energy level in the laser medium. The rise and fall time of the pulse become simultaneously shorter, leading to the decrease of pulse width and the increase of repetition rate. To further analyze the evolution of the pulse circulating the laser cavity with the changing pump power, the relation of the repetition rate and pulse width as a function to pump power is illustrated in Figure 9. The graph shows that the repetition rate is proportional to the input power where the repetition rate increases from 12.6 kHz to 177.7 kHz with increasing pump power. As observed, the pulse width is inversely proportional to the input power where the pulse width is decreased from 9.33  $\mu$ s to 1.32  $\mu$ s. From the measured pulse repetition rate, pulse width and average output power, we calculated the pulse energy and peak power, and the data is tabulated in Figure 10. As shown, the calculated pulse energy decreased proportionally with the input pump power from 11.2 nJ to 0.3 nJ. These values are considered higher as compared to previous reported work [8]. The calculated peak power recorded a different trend with increment from 1.13 mW to the highest of 1.62 mW slightly better than [8] and then started to decrease when the input pump power was tuned from threshold pump power to the maximum pump power. The fluctuation of the pulse energy and peak power is also reported in [12]. One way to reduce the fluctuation is by using higher ratio of output coupler as in their case from 90/10 output coupler to 50/50 output coupler [12].

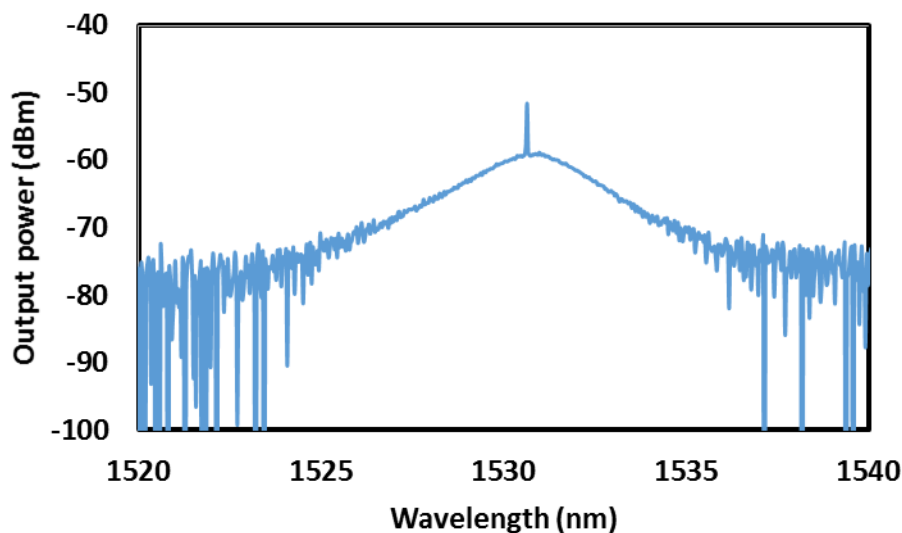


Figure 6. Central wavelength of 1531 nm

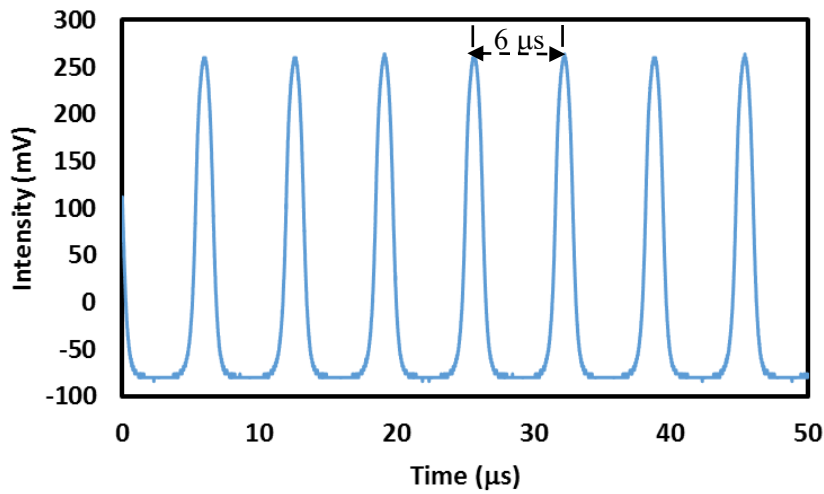


Figure 7. Pulse train with repetition rate of 166 kHz at 126 mW

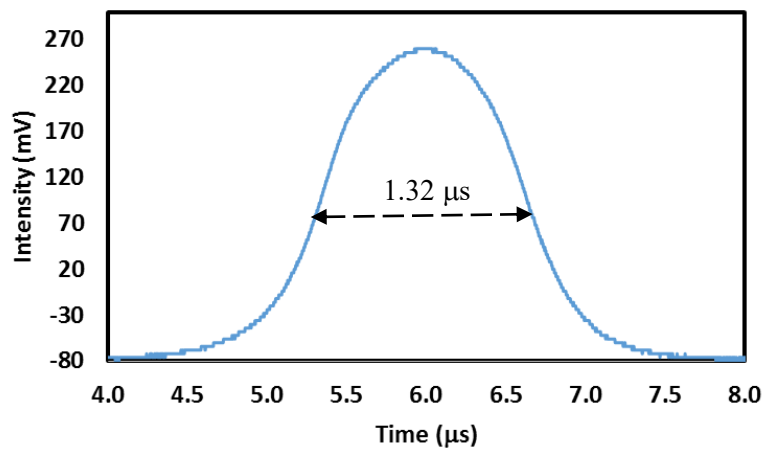


Figure 8. Single pulse envelope with 1.32 μs pulse width at 126 mW

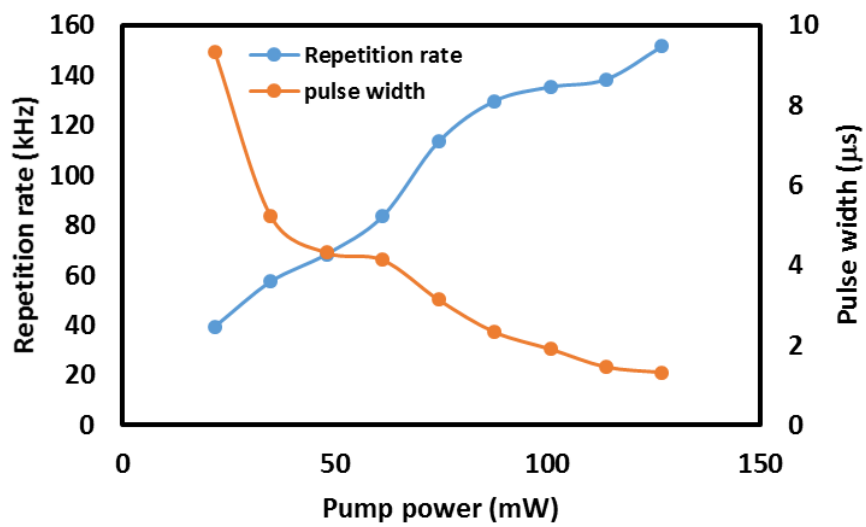


Figure 9. Repetition rate and pulse width versus pump power

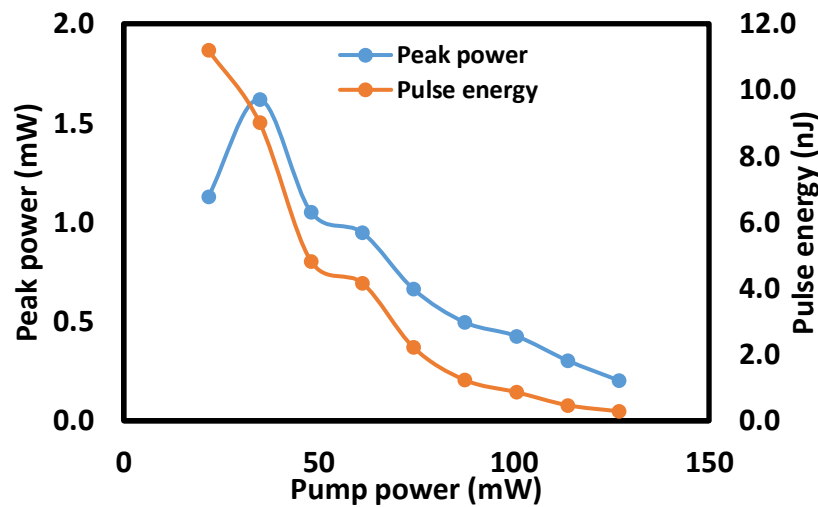


Figure 10. Peak power and pulse energy versus pump power

To investigate the laser stability, we measure its corresponding radio frequency (RF) spectrum. As can be seen in Figure 11, the signal-to-noise ratio (SNR) of our fiber laser is over 49 dB, indicating that the Q-switched pulse operates in a relatively stable regime. Moreover, the SNR recorded in this work is slightly better than the reported Q-switched in previous work [7-8,14] by using the Bismuth (III) Telluride based passive saturable absorber. Table 1 shows some of the previous works that also uses Bi<sub>2</sub>Te<sub>3</sub>-based passive SA operating in 1.5  $\mu$ m region.

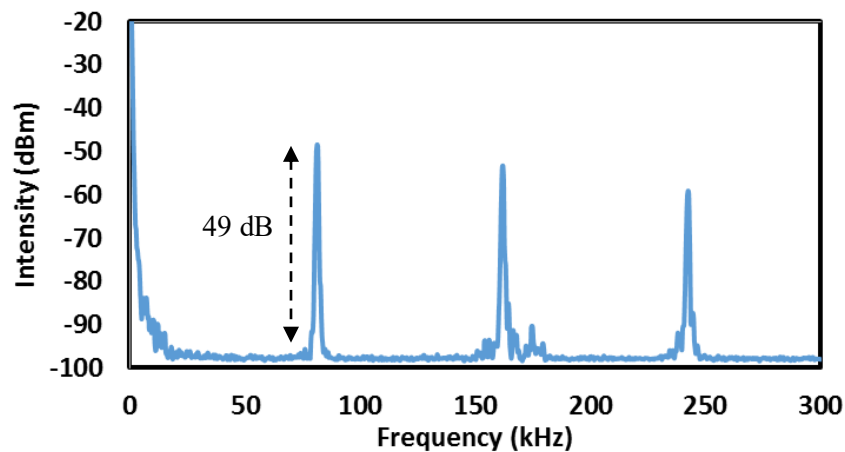


Figure 11. First beat note of 49 dB with frequency of 81.3 kHz

Table 1. Er-doped Q-switched fiber lasers employing Bi<sub>2</sub>Te<sub>3</sub> based passive SA.

Repetition rate (kHz)	Pulse width ( $\mu$ s)	Peak power (mW)	Pulse energy (nJ)	SNR (dB)	Refs
2.2-12.8	13	20	1500	36.4	[7]
12.6-177.7	0.2	1.3	7.5	47	[8]
2.6-12	9.5	120	4	40	[14]
40-166	1.32	1.62	11.2	49	This work

## 5. Conclusion

A simpler approach in the fabrication process of Bi<sub>2</sub>Te<sub>3</sub>-PVA as passive Q-switcher has been demonstrated in this work. The Bi<sub>2</sub>Te<sub>3</sub> was dispersed in PVA by solution casting approach and then dried at ambient temperature to develop a Bi<sub>2</sub>Te<sub>3</sub>-PVA film. Promisingly, the proposed Q-switcher managed to produce a tunable repetition rate from 40 kHz to 166 kHz with the shortest pulse width of 1.32 μs. Maximum instantaneous output peak power and pulse energy of 1.62 mW and 11.2 nJ respectively, have been recorded throughout the experiment.

## References

- [1] Soffer B 1964 *Journal of Applied Physics* **35** 2551
- [2] Woodward R and Kelleher E 2015 *Applied Sciences* **5** 1440-1456
- [3] Zhang H, Liu C, Qi X, Dai X, Fang Z and Zhang S 2009 *Nature Physics* **5** 438-442
- [4] Ren L, Qi X, Liu Y, Hao G, Huang Z, Zou X et al. 2012 *Journal of Materials Chemistry* **22** 4921
- [5] Zhao C, Lu S, Qi X, Zhang H, Wen S and Tang D 2013 *Applied Physics Letters* **103** 106101
- [6] Lee J, Koo J, Chi C and Lee J 2014 *Journal of Optics* **16** 085203
- [7] Chen Y, Zhao C, Chen S, Du J, Tang P, Jiang G et al. 2014 *IEEE Journal of Selected Topics in Quantum Electronics* **20** 315-322
- [8] Wu M, Chen Y, Zhang H et al. 2014 *IEEE Journal of Quantum Electronics* **50** 393-396
- [9] Lee J, Jung M, Koo J et al. 2015 *IEEE Journal of Selected Topics in Quantum Electronics* **21** 31-36
- [10] Li J, Luo H, Wang L et al. 2015 *Optics Letters* **40** 3659-3662
- [11] Liu H, Zheng X, Liu M, Zhao N, Luo A, Luo Z et al. 2014 *Optics Express* **22** 6868
- [12] Xin H, Hang Z, Wei L, Rongfei W, Jianrong Q, Mei Z and Bin H 2015 *Scientific Reports* **5** 15868
- [13] Russo V, Bailini A, Zamboni M, Passoni M, Conti C, Casari C S, Li Bassi A and Bottani C E 2008 *Journal of Raman Spectroscopy* **14** 205-210
- [14] Chen, S. Q. et al. 2014 Stable *IEEE Photonic. Tech. L.* **26** 987-990